DOI: 10.1007/s11099-018-0832-6 PHOTOSYNTHETICA 56 (4): 1378-1386, 2018

# Foliar exposure of grapevine (*Vitis vinifera* L.) to $TiO_2$ nanoparticles under field conditions: Photosynthetic response and flavonol profile

P. TESZLÁK[*§], M. KOCSIS[**§], A. SCARPELLINI[***], G. JAKAB[*,**], and L. KŐRÖSI[*,+]

*Research Institute for Viticulture and Oenology, University of Pécs, Pázmány P. u. 4, H-7634 Pécs, Hungary*[*]
*Department of Plant Biology, University of Pécs, Ifjúság u. 6, H-7624 Pécs, Hungary*[**]
*Electron Microscopy Facility, Istituto Italiano di Tecnologia, via Morego 30, 16163 Genova, Italy*[***]

## Abstract

In the past decade, utilization of nanostructured materials has increased intensively in a wide range of applications. Titanium dioxide nanoparticles ($TiO_2$ NPs), for instance, can be applied for the inactivation of various pathogens through photo-induced generation of reactive oxygen species. Although $TiO_2$ NPs with high antimicrobial activity are of great importance, in practice, their phytotoxic effects have not yet been fully clarified. In this study, we investigated the potential phytotoxicity of $TiO_2$ NPs on grapevine (*Vitis vinifera* L.) under field conditions. After foliar exposure, two particularly stress-sensitive parameters, photosynthetic function and the flavonol profile, were examined. Micro- and macroelement composition of the leaves was also studied by ICP-AES measurements. We found that $TiO_2$ NPs significantly decreased the net $CO_2$ assimilation and increased stomatal conductance, indicating metabolic (nonstomatal) inhibition of the photosynthesis. The lower electron transport rate and lower nonphotochemical quenching in treated leaves are indicative of diminished photoprotective processes.

*Additional key words*: chlorophyll fluorescence; flavonols; grapevine; macroelement; nanotoxicity; photosynthesis; titanium dioxide.

## Introduction

During the past few decades, nanotechnology has attracted a huge attention due to revolutionary new applications in numerous scientific fields. This includes a broad range of engineered nanomaterials with specific physicochemical properties. The use of such nanomaterials in applications will, unavoidably, lead to their interactions with the environment and various living organisms. Since NPs have a high specific surface area and are generally highly reactive, they can exhibit an increased uptake, accumulation, and impact on plants and humans (Yokel *et al.* 2011, Zhao *et al.* 2016, Fadeel *et al.* 2017). The mechanism of toxicity and long-term impacts of these NPs are still not exactly understood, and consequently further investigations are required to explore and clarify them.

Based on its excellent physicochemical properties, $TiO_2$ is a widely used material in numerous sectors of industry. It is most widely used as a white pigment. Foods (*e.g.* candies, sweets, and chewing gums) as well as personal care products (sun creams, cosmetics, tooth-pastes) and pharmaceuticals, just to name a few, often contain $TiO_2$ (Weir *et al.* 2012). As a photocatalyst, $TiO_2$ can also be utilized for water and air purification and for creating antibacterial surfaces (Hashimoto *et al.* 2005). The photoactivity and antimicrobial ability of $TiO_2$ are based on the photoinduced charge separation and the subsequent redox reactions in which the photo-generated

*Received* 24 September 2017, *accepted* 15 January 2018, *published as online-first* 21 June 2018.
[+]Corresponding author; phone: 0036 72517933, e-mail: korosi.laszlo@pte.hu
*Abbreviations*: $C_i$ – intercellular $CO_2$ concentration; $E$ – transpiration rate; ETR – electron transport rate; $F_0'$ – minimal fluorescence yield at the light-adapted state; $F_m'$ – maximal fluorescence yield at the light-adapted state; $F_s$ – steady-state fluorescence yield; $g_s$ – stomatal conductance; HPLC – high-performance liquid chromatography; DAD – diode array detector; ICP-AES – inductively coupled plasma atomic emission spectroscopy; NPQ – nonphotochemical quenching; $q_P$ – photochemical quenching coefficient; $P_N$ – net photosynthetic rate; RLC – rapid light curve; ROS – reactive oxygen species; TEM – transmission electron microscopy; $TiO_2$ NPs – titanium dioxide nanoparticles; UVA/B – ultraviolet A and B radiation; $WUE_i$ – intrinsic water-use efficiency (= $P_N/g_s$); XRD – X-ray diffraction; $\Phi_{PSII}$ – effective quantum yield of PSII photochemistry.
*Acknowledgments:* This paper was supported by the János Bolyai Research Scholarship of the Hungarian Academy of Sciences. The authors thank Dr. Marcel A. K. Jansen (University College Cork, School of Biological, Earth & Environmental Sciences) for his helpful remarks and comments.
[§]co-first authorship

charge carriers (electrons and holes) react with the donor (*e.g.* $H_2O$) or acceptor (*e.g.* $O_2$, $H_2O_2$) molecules adsorbed on the surface of $TiO_2$ NPs, thus produce reactive oxygen species (ROS) (Kőrösi *et al.* 2013, 2016). The basic reactions are as follows:

$$TiO_2 + h\nu \rightarrow e_{CB}^- + h_{VB}^+ \quad (1)$$
$$e_{CB}^- + O_2 \rightarrow O_2^{\bullet -} \quad (2)$$
$$h_{VB}^+ + H_2O \rightarrow OH^\bullet + H^+ \quad (3)$$
$$H_2O_2 + e_{CB}^- \rightarrow OH^\bullet + OH^- \quad (4)$$
$$H_2O_2 + h_{VB}^+ + 2OH^- \rightarrow O_2^{\bullet -} + 2H_2O \quad (5)$$

Because of their photoinduced reactivity, $TiO_2$ NPs can be exploited as a potential antimicrobial agent on leaves. Moreover, since ROS have signalling role, $TiO_2$ NPs can influence the resistance of the plants against pathogens and can also affects the abiotic stress responses (Qi *et al.* 2013).

In addition to the toxicity of engineered nanomaterials towards humans, a large number of studies have focused on phytotoxicity of $TiO_2$ NPs (Khan *et al.* 2017). For phytotoxicity tests, a large variety of model plants, such as tomato, wheat, soybean, parsley, spinach, corn, fennel, and cucumber, was used. Overall, the effects of nanoparticles are very diverse. Depending on the physiological processes studied, both negative and positive impacts were observed. For example, $TiO_2$ NPs could promote the light absorption by the chloroplast in *Arabidopsis*, regulate the distribution of light energy from PSI to PSII, and accelerate the transformation from light energy to electric energy, water photolysis, and oxygen evolution (Ze *et al.* 2011). In contrast, Du *et al.* (2011) found that $TiO_2$ NPs negatively affect the growth of wheat including biomass accumulation and soil enzyme activities. Castiglione *et al.* (2011) demonstrated that $TiO_2$ NPs induced genotoxic effect in *Vicia narbonensis* L. and *Zea mays* L. In other studies, NPs did not show significant effects on plant growth. Song *et al.* (2013) reported that $TiO_2$ NPs were not toxic *in vitro* or *in situ* for oilseed rape, lettuce, and kidney bean. In another study, Jacob *et al.* (2013) revealed that $TiO_2$ NPs did not affect biomass production of several plant species, such as *Phaseolus vulgaris, Triticum aestivum, Rumex crispus*, and *Elodea canadensis*, but significantly increased Ti adsorption and uptake in roots and translocation of Ti into shoots. For maize and soybean plants, Burke *et al.* (2014) found that $TiO_2$ NPs did not have significant effects on growth, nutrient content, or the composition of bacterial communities within the rhizosphere. Most studies on phytotoxicity focus on standardised assays, usually on germination and plant growth. Such studies typically investigate the effects of NPs-treated soil and/or nutrient solution on plants. Only a few studies can be found in the literature wherein solely foliar exposure was applied (Ze *et al.* 2011, Gao *et al.* 2013, Qi *et al.* 2013, Larue *et al.* 2014, Raliya *et al.* 2015). Moreover, in spite of the fact that $TiO_2$ is photo-reactive (*i.e.* photocatalyst), the applied nanomaterials are generally not exposed to sunlight, including reactive UV radiation.

Grape is one of the most economically important fruit crops worldwide which is planted at above 7 million hectares. Based on the planted area, grape belongs to the first 25 fruit crop in the world (Keller 2010). It is grown mostly for making wines, raisins, and as fresh fruit (table grapes). In this study, a well-characterized nanostructured $TiO_2$ with high photocatalytic activity was used for the foliar exposure of the world-wide cultivated grapevine variety 'Cabernet Sauvignon'. In the field experiment, the plants were exposed to natural sunlight. After $TiO_2$ NPs treatment, photosynthesis was monitored by means of leaf gas exchange and chlorophyll (Chl) *a* fluorescence. The main flavonol profile of grapevine leaves was determined by high-performance liquid chromatography (HPLC), to reveal possible changes among these nonenzymatic antioxidants. Polyphenols are a large family of secondary metabolites including flavonoids like flavonols, anthocyanins, flavanols, and non-flavonoids like phenolic acids and stilbens (Flamini and Traldi 2010). Most of these polyphenols, mainly flavonoids, outperform well-known antioxidants, because of their strong capacity to donate electrons or hydrogen atoms (Hernández *et al.* 2009). Since grapevine leaves are rich in polyphenols, these secondary metabolites may contribute significantly to the nonenzymatic defense. Indeed, these compounds are sensitive indicators of different abiotic and biotic stresses (Chacón *et al.* 2009, Taware *et al.* 2010, Anđelković *et al.* 2015).

This is the first study in which the potential phytotoxicity of the $TiO_2$ NPs was investigated over a longer period (three weeks) on grapevine in the presence of UVA/B radiation. Two particularly stress-sensitive parameters, photosynthetic function and the flavonol profile, were examined to reveal potential impacts of photo-excited $TiO_2$ NPs under natural light conditions.

## Materials and methods

**Chemicals and reagents**: Acetonitrile and methanol (*LiChrosolv® Reag. Ph Eur, Merck*, Germany) were gradient grade for liquid chromatography. Orthophosphoric acid (85%) and ethanol (96%, purchased from *VWR*) were of analytical reagent grade. Reference substances of quercetin 3-O-rutinoside, quercetin 3-O-glucoside, quercetin 3-O-glucuronide, kaempferol 3-O-glucoside, and kaempferol 3-O-glucuronide were obtained from *Extrasynthese* (Genay, France). Ultrapure water system (*LaboStar™ 7 TWF-UV*, Germany) was used to obtain high purity water.

**Plant material and experimental design**: Two-year-old plants of *Vitis vinifera* L. (cv. 'Cabernet Sauvignon') were investigated in a large-pot experiment under field conditions. Vines were grafted on 'T5C' rootstock. Plants

were grown in large plastic pots (37 cm in diameter, 27 cm high, with a volume of 20 L). The study was carried out at the central station of the Research Institute for Viticulture and Oenology (University of Pécs, Hungary) on south-facing slopes of the Mecsek Hills (46º04'N, 18º11'E, 150 m a.s.l.). The site receives precipitation of 782 mm per year, 2,021 h of sunshine annually, and has an annual mean temperature of 11.6°C according to the vineyard meteorological records for the period 1950 and 2010 (Teszlák *et al.* 2013). During the experiments the meteorological data were monitored using the *WS600* automatic weather station (*Lufft GmbH*, Germany). The obtained data (natural broadband UV, precipitation, temperature, and relative humidity) are shown in Fig. 1S and Table 1S (*supplements available online*). The climatic conditions of experimental period were described by two bioclimatic indices. Huglin and BBL-hydrothermic indices were 2,241 and 9,277, respectively (Lorenzo *et al.* 2012). These indices showed favourable growing conditions to the grapevine development during a vegetation period. Twenty vine stocks were planted in May 2016 into the pots filled with natural soil (brown forest soil mixed with clay; soil samples were collected from our vineyard close to the experimental site). From this pool of plants, three individual plants with similar developmental characteristics were chosen for the $TiO_2$ NPs treatment. All pots were irrigated daily and supplemented once per month with 20 g of complex fertilizer (*Volldünger 14-7-21 NPK, Kwizda*, Austria).

**Characterizations of $TiO_2$ NPs**: X-ray diffraction (XRD) patterns were collected using CuKα radiation by a *Rigaku SmartLab* X-ray diffractometer operating at 40 kV and 150 mA. The mass fraction of the rutile phase ($f_r$) was calculated *via* the following relationship (Yu *et al.* 2006):

$$f_r = \frac{1.26\, I_r}{I_a + 1.26\, I_r}$$

where $I_a$ and $I_r$ are the area of (101) and (110) diffraction peaks of anatase and rutile, respectively. Transmission electron microscopy (TEM) images were obtained with a *JEM-1011* (*JEOL,* Japan) electron microscope at an accelerating voltage of 100 kV. Inductively coupled plasma atomic emission spectrometry (ICP-AES) measurements were performed on a *ICPE-9000* instrument (*Shimadzu*, Japan). Prior to the elemental analysis, the dried leaves were digested using a *Multiwave 3000* (*Anton Paar*, Austria) microwave system. For Ti content determination, the crushed leaves were combusted and the resulting ignition residues were heated with anhydrous NaOH up to redness in a Ni crucible. The cooled melts were dissolved completely in water by the addition of 96% $H_2SO_4$. Finally, the obtained solutions were analysed by ICP-AES.

**Leaf gas-exchange measurements** were conducted *in situ* on attached leaves using an infrared open-system portable *LCA-4* gas analyser (*ADC BioScientific Ltd.*, Hoddesdon, UK) with nine replicates of leaves per sampling. Mature and healthy sun-adapted leaves from the $5^{th}$–$12^{th}$ nodes were used for analysis. Measurements of the maximum photosynthetic activity of leaves were carried out between 10:00 and 11:30 h local time, at PAR of 1,500–1,800 μmol(photon) $m^{-2}$ $s^{-1}$ under normal atmospheric $CO_2$ concentration. The leaf surface temperature was 25°C (in September) or 17°C (in October), under 0.38–0.42 kPa vapour pressure deficit. We determined the net $CO_2$ assimilation ($P_N$), the rate of transpiration ($E$), the stomatal conductance ($g_s$), the value of partial pressure of intercellular $CO_2$ (mesophyll conductance) ($C_i$), and intrinsic water-use efficiency ($WUE_i$). The PAR incidence on leaves was always higher than 1,500 μmol(photon) $m^{-2}$ $s^{-1}$, which is considered to be in excess of the incidence required for photosynthetic saturation in grapevine (Flexas *et al.* 2002). $P_N$, $E$, $g_s$, and $C_i$ were calculated using the equations of von Caemmerer and Farquhar (1981). The $P_N/g_s$ ratio was used to indicate $WUE_i$, according to Iacono *et al.* (1998). Gas-exchange measurements were performed five times after the NPs treatment, between 21 September and 13 October ($n = 9$) during the preharvest phenological period.

**Leaf chlorophyll (Chl) fluorescence measurements**: Following the gas-exchange measurements, the same attached leaves were used for analysis of Chl *a* fluorescence with a pulse amplitude modulation fluorometer *PAM-2100* (*Heinz Walz GmbH,* Effeltrich, Germany) connected to a notebook computer. For the nondestructive *in situ* measurements we used the 'rapid light curves' (RLCs) option of the *PamWin* data acquisition software with pre-programmed operating parameters (*PamWin v 1.17, Heinz Walz GmbH,* Effeltrich, Germany). Each RLC consists of 10 illumination steps with increasing PAR between 0 and 2,600 μmol(photon) $m^{-2}$ $s^{-1}$. Effective quantum yield of PSII ($\Phi_{PSII}$), photochemical quenching ($q_P$), relative electron transport rate (ETR), and regulated nonphotochemical quenching (NPQ) parameters were recorded during each steps of RLC (Maxwell and Johnson 2000). The effective quantum yield of PSII reaction centres ($\Phi_{PSII}$) and photochemical quenching parameter ($q_P$) were calculated as $(F_m' - F_s)/F_m'$ and $(F_m' - F_s)/(F_m' - F_0')$, respectively (Genty *at al.* 1989).

**$TiO_2$ treatment of grapevine leaves**: Nine healthy fully developed and sun-adapted leaf samples were investigated at each time-point in the experiment. The samples originated from three different plants (three control and three treated leaves per vine stock). For the foliar exposures, 100 mg of *Degussa P25* $TiO_2$ was dispersed in 100 ml of deionized water (Gao *et al.* 2013) by using an ultrasonic bath for 15 min. The dispersion was sprayed homogenously on to the adaxial surface of the leaves, after which the surface was allowed to dry slowly. No surfactant or additives were applied in the dispersion. After drying of $TiO_2$ dispersion, NPs remained on leaves even following

several rain showers, indicating that nanoparticles adhered well to the surface. All nondestructive field measurements were done on the same individually identified leaf samples.

**Sample preparation and extraction**: Grapevine leaves were dried to a constant, reproducible mass at room temperature in dark. These air-dried samples were grounded in a porcelain mortar, and then extracted with 96% (v/v) ethanol solution. The extraction procedure was as follows: 500 mg of powder sample was placed in a plastic tube. 10 ml of ethanol was added, and subsequently sonicated in water bath for 45 min. The resulting suspension was centrifuged at 20,660 × *g* and the supernatant was filtered through a 0.45 µm PTFE (*FilterBio®, Labex Ltd.*, Hungary) syringe filter.

**High-performance liquid chromatography analysis (HPLC-DAD)**: Chromatographic analysis was performed on a *PerkinElmer Series 200 HPLC* system consisting of a vacuum degassing unit, quaternary pump, autosampler, column thermostat, and a diode array detector (DAD). HPLC separations were achieved by using a *Phenomenex Kinetex® 2.6 µm XB-C18 100 Å*, 100 × 4.6 mm column. Column temperature was maintained at 25°C. Mobile phase was composed of (A) 50 mM phosphoric acid and (B) a mixture of 100 mM phosphoric acid and acetonitrile (1:1) at a flow rate of 1 ml $min^{-1}$. For the separation, the elution program (Table 2S, *supplement available online*) was comprised of subsequent isocratic and both linear and nonlinear (with curved profile) gradient steps. A volume of 5 µl of ethanolic extract was injected to HPLC system and the absorbance was monitored at 350 nm.

**Statistical analyses** were carried out using *Excel®* (*Microsoft Corp*., Redmond, USA). Standard deviation and paired *t*-tests were calculated on all data sets. Results were considered statistically significant at $P<0.05$. The correlation analysis between elemental composition and photosynthetic parameters was performed using linear regression with significant differences at $P<0.05$.

## Results and discussion

**Crystal phase, particle size and morphology of $TiO_2$ NPs**: For the treatment of 'Cabernet Sauvignon' leaves, an aqueous dispersion of *Degussa P25* $TiO_2$ was used. Due to its excellent photocatalytic activity *P25* is frequently studied as a reference photocatalyst for various dye degradation reactions, or the inactivation of bacteria, viruses, and fungi (Carp *et al.* 2004, Ohtani *et al.* 2010). *P25* $TiO_2$ consists of anatase and rutile crystal phases as presented by the XRD pattern in Figure 1*A*. The calculated crystalline phase composition revealed that the predominant phase is anatase (88 w/w%) while it contains 12 w/w % rutile. The average sizes of anatase and rutile crystallites calculated *via* the Scherrer equation from the corresponding (101) and (110) reflections were 27.1 and 38.9 nm, respectively. TEM image (Fig. 1*B*) with the corresponding size distribution (Fig. 2S, *supplement available online*) shows polymorph and polydispersed $TiO_2$ NPs with a mean particle diameter of ~28 nm.

**Effects of $TiO_2$ NPs on leaf gas-exchange parameters**: Similar $P_N$ and $g_s$ values were observed for both control and treated leaves during the first 6 d following the NPs treatment (Fig. 2*A*,*B*). However, $TiO_2$ treatment resulted in significantly lower $P_N$ values on the $10^{th}$ day, and a further marked decrease on day 23. It should be noted that the leaf surface temperature gradually decreased according to the field conditions (Table 1S), leading to lower $P_N$ values independently from the treatment (Fig. 2*A*). Compared with the control leaves, $P_N$ was 53% lower at the last sampling date. In addition, treated leaves showed extremely high $g_s$ values, which were 82% higher than those of the control ones (Fig. 2*B*). In spite of the grapevine leaves being hypostomatic, the adaxial treatment with

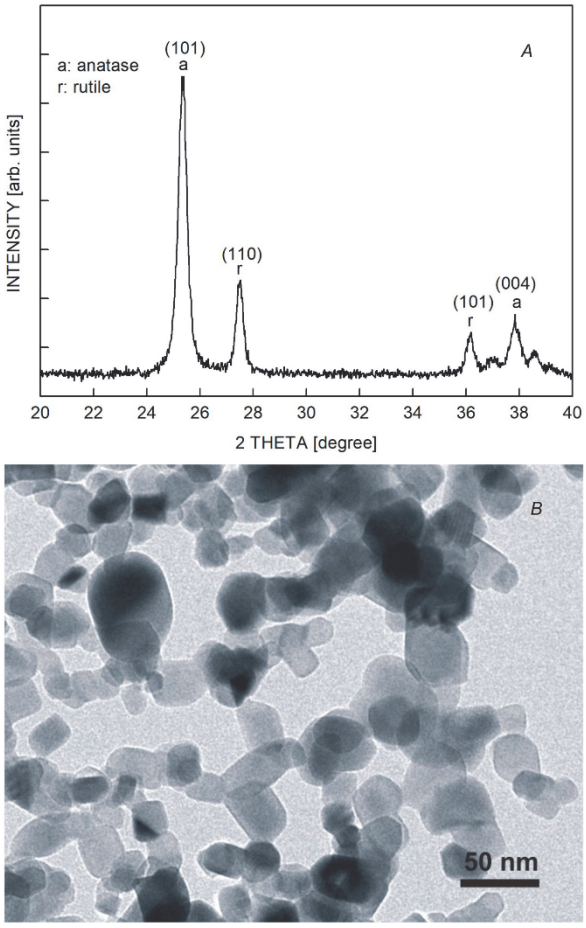


Fig. 1. (*A*) X-ray diffraction pattern and (*B*) transmission electron microscope image of P25 $TiO_2$ NPs.

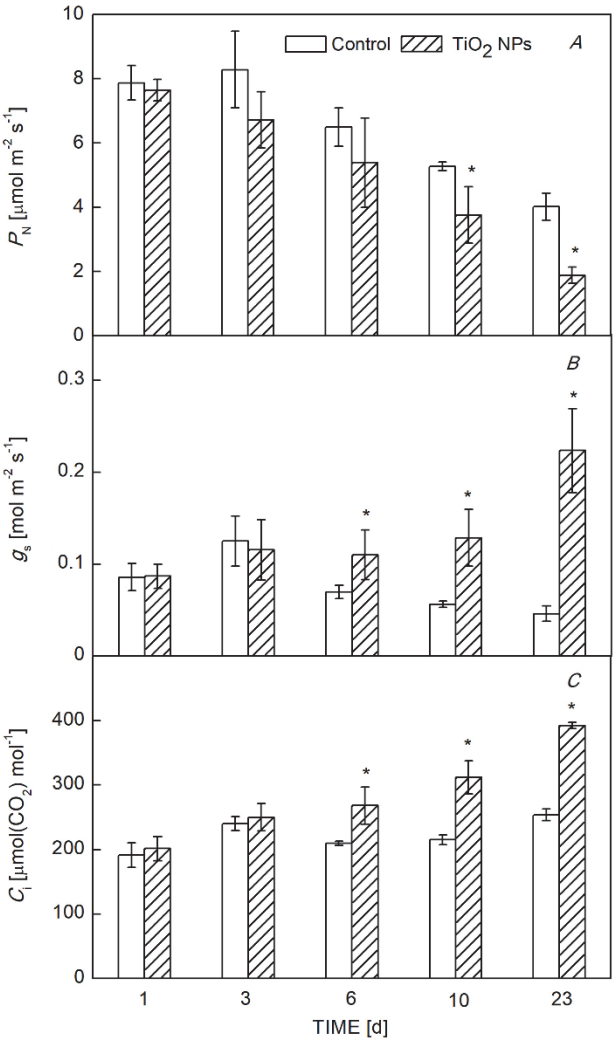


Fig. 2. Effect of $TiO_2$ NPs treatment on the photosynthetic gas-exchange parameters of grapevine leaves: (*A*) Net $CO_2$ assimilation rate ($P_N$), (*B*) stomatal conductance ($g_s$), and (*C*) intercellular $CO_2$ concentration ($C_i$). Data are the means of nine replicates with standard deviation shown by vertical bars. * – significant difference ($P \leq 0.05$).

$TiO_2$ NPs triggered the opening of stomata located at the abaxial leaf surface. The intercellular $CO_2$ concentration is presented in Fig. 2*C*. Treated leaves exhibited higher $C_i$ values after 6, 10, and 23 d. The highest mean value of $C_i$ was close to 400 µmol mol$^{-1}$ indicating a strong decrease of mesophyll conductance of $CO_2$ resulting in its accumulation in intercellular spaces. In $C_3$ plants, like grapevines, $CO_2$ can diffuse from intercellular air spaces into photosynthesizing mesophyll cells across the cell membrane, the cytosol, and the chloroplast outer membrane to reach the site of carboxylation (Flexas *et al.* 2013). Consequently, the significantly higher $C_i$ values may refer to the decreased $CO_2$ transport into the chloroplast caused by $TiO_2$ NPs. In summary, the high $g_s$ and high $C_i$ values along with the reduced $P_N$ revealed a definitive metabolic inhibition of the photosynthesis.

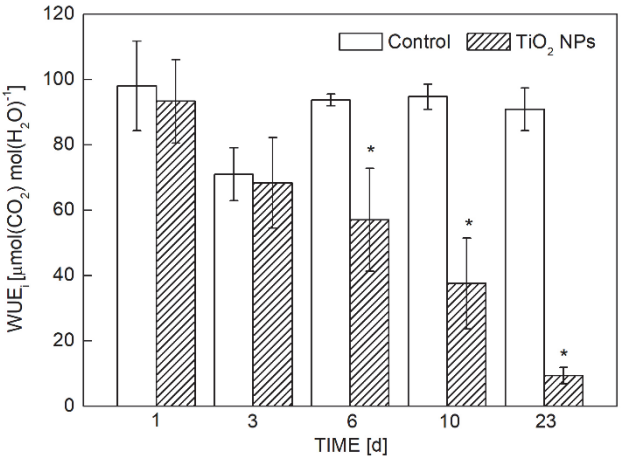


Fig. 3. Effect of $TiO_2$ NPs treatment on the intrinsic water-use efficiency ($WUE_i = P_N/g_s$) of grapevine leaves. Data are the means of nine replicates with standard deviation shown by vertical bars. * – significant difference ($P \leq 0.05$).

$TiO_2$ NPs also induced changes in $WUE_i$. There was no considerable difference in $WUE_i$ at the first and second sampling dates (Fig. 3) when samples exhibited typical $WUE_i$ values of grapevine cultivars (Tomás *et al.* 2014, Tortosa *et al.* 2016). After six-day $TiO_2$ exposure, $WUE_i$ decreased markedly (40% lower) because of the unchanged $P_N$ and higher $g_s$ values. After 10 and 23 d, the decrease of $WUE_i$ continued (60 and 90%, respectively). Such extremely low $WUE_i$ values were previously observed in drought-stressed grapevine cultivars (Medrano *et al.* 2015). Low $WUE_i$ has also been reported for nano-anatase $TiO_2$- treated *Ulmus elongata* seedlings (Gao *et al.* 2013). In agreement with our results, these authors also observed significantly higher $g_s$ values along with low $P_N$ for $TiO_2$-treated seedlings.

**Effect of $TiO_2$ NPs on leaf Chl *a* fluorescence parameters**: The Chl fluorescence parameters are sensitive indicators of photoinhibition and photodamage caused by excess light energy in grapevine chloroplasts. The light-response curves recorded after three weeks of $TiO_2$ NPs exposure are presented in Fig. 4. Control and treated leaves exhibited similar $\Phi_{PSII}$ and $q_P$ over the whole range of PAR [0–2,600 µmol(photon) m$^{-2}$ s$^{-1}$] suggesting that photocatalytically active $TiO_2$ NPs did not cause damage to PSII during the experimental period (Fig. 4*A,B*). Mean values of the linear electron transport rate (ETR) of PSII were light-intensity dependent during the RLC analysis. At lower light intensities [0–1,000 µmol(photon) m$^{-2}$ s$^{-1}$], there was no significant difference in ETR between control and treated leaves, but above 1,500 µmol(photon) m$^{-2}$ s$^{-1}$, a 27% lower ETR was measured for NPs-treated leaves (Fig. 4*C*). Both the lower ETR and $P_N$ suggested a slight inhibition of photosynthetic apparatus through nonstomatal limitation process. The disruption of ETR or photosynthesis is more pronounced at high irradiance which may relate to the intensity of the charge

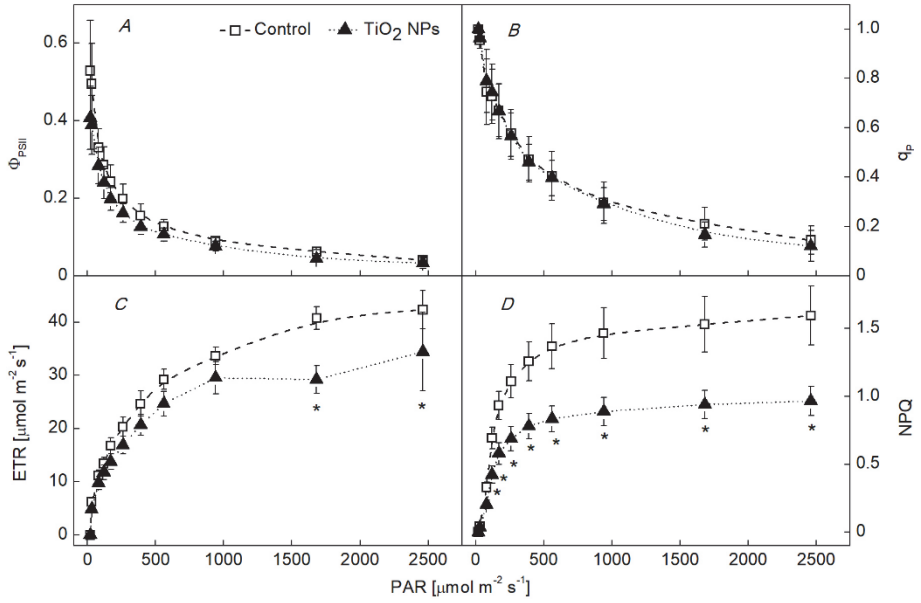


Fig. 4. Effect of $TiO_2$ NPs treatment on the (*A*) quantum yield of PSII ($\Phi_{PSII}$), (*B*) photochemical quenching ($q_P$) of variable Chl *a* fluorescence, (*C*) relative electron transport rate (ETR), and (*D*) regulated energy dissipation of PSII (NPQ) of grapevine leaves. Data are the means of nine replicates with standard deviation shown by vertical bars. * – significant difference ($P \leq 0.05$).

Table 1. Correlation analysis between elemental composition and photosynthetic parameters of Cabernet Sauvignon leaves. Data are means ± SD ($n$ = 9); significant correlation between gas-exchange parameters is indicated with asterisks. (* – significant at $P \leq 0.05$ level, ** – highly significant at $P \leq 0.01$ level, and n.s. – not significant). The elements are expressed in [mg $kg^{-1}$(DW)].

| | K | Ca | Mg | P | B | Fe | Mn | Cu | Zn | Ti |
|---|---|---|---|---|---|---|---|---|---|---|
| Control | 10,251 ± 428 | 22,877 ± 1,237 | 1,575 ± 112 | 2,126 ± 229 | 13 ± 1 | 82 ± 1 | 99 ± 7 | 104 ± 18 | 44 ± 2 | n.d. |
| $TiO_2$ NPs treated | 16,166 ± 1,423 | 25,729 ± 1,672 | 1,809 ± 104 | 3,214 ± 413 | 22 ± 4 | 83 ± 3 | 111 ± 7 | 116 ± 29 | 37 ± 8 | 276 ± 26 |
| $E$ | * | n.s. | n.s. | * | * | n.s. | n.s. | n.s. | n.s. | ** |
| $g_s$ | * | n.s. | n.s. | * | n.s. | n.s. | n.s. | n.s. | n.s. | ** |
| $WUE_i$ | * | n.s. | n.s. | * | n.s. | n.s. | n.s. | n.s. | n.s. | ** |

carrier generation (and the subsequent charge-transfer processes) according to Eq. 1. Based on the measured lower $P_N$, ETR, and the higher $C_i$, treated leaves had a higher photorespiration. Further studies are necessary to clarify the effect of $TiO_2$ NPs treatment on photo-respiration and dark respiration in grapevine leaves.

NPQ of treated and control leaves differed significantly in the PAR range of RLC (Fig. 4*D*). $TiO_2$ NPs induced 40% lower NPQ values both at lower and higher irradiance. In general, NPQ reflects heat-dissipation of excitation energy under excess radiation energy, and a higher level of NPQ is a well-known indicator of different stress situations caused by excess light, heat or drought stress in grapevine leaves. Increased NPQ is indicative of photoprotective processes such as thermal dissipation at the antenna level in chloroplasts (Medrano *et al.* 2002). According to our measurements, treated leaves with lower NPQ values partially lost their ability to prevent photodamage after the three weeks $TiO_2$ exposure.

**Macro- and microelemental analysis by ICP-AES**: The main macro- (Mg, P, K, Ca), microelements (B, Zn, Mn, Fe, Cu), and Ti in leaves were determined after three weeks of $TiO_2$ exposure by inductively coupled plasma atomic emission spectroscopy (ICP-AES). The results are listed in Table 1. The total (including both adhered and absorbed) Ti content of leaves was 276 ± 26 mg $kg^{-1}$(DW). The results show that K, Ca, Mg, and P contents were significantly higher in the $TiO_2$ NPs exposed leaves, while the concentration of the measured microelements, with exception of B, was not influenced by the NPs treatment (Table 1). $TiO_2$ NPs treatment increased on average the K concentration from 10,251 mg $kg^{-1}$(DW) to 16,166 mg $kg^{-1}$(DW), while P content increased from 2,126 mg $kg^{-1}$(DW) to 3,214 mg $kg^{-1}$(DW). In spite of the different treatment procedure, Servin *et al.* (2013) also found that cucumber fruits from plants treated with $TiO_2$ NPs have a higher content of the primary macronutrients K and P. These authors cultivated the plants in soil treated with $TiO_2$ and demonstrated that the nanoparticles translocated from roots to fruits. We found that $TiO_2$ NPs did not

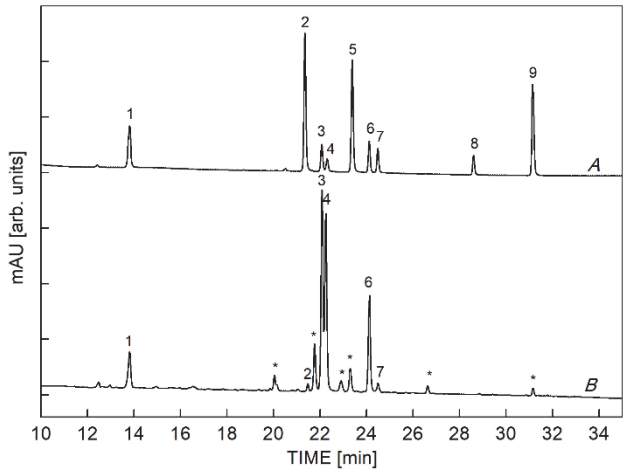


Fig. 5. HPLC-DAD chromatograms of (*A*) a mixture of different polyphenols and (*B*) ethanolic extract of control Cabernet Sauvignon leaves. (1) caftaric acid (2) quercetin-3-O-rutinoside, (3) quercetin-3-O-glucoside, (4) quercetin-3-O-glucuronide, (5) kaempferol-3-O-rutinoside, (6) kaempferol-3-O-glucoside, (7) kaempferol-3-O-glucuronide, (8) quercetin, and (9) kaempferol. * – unknown components

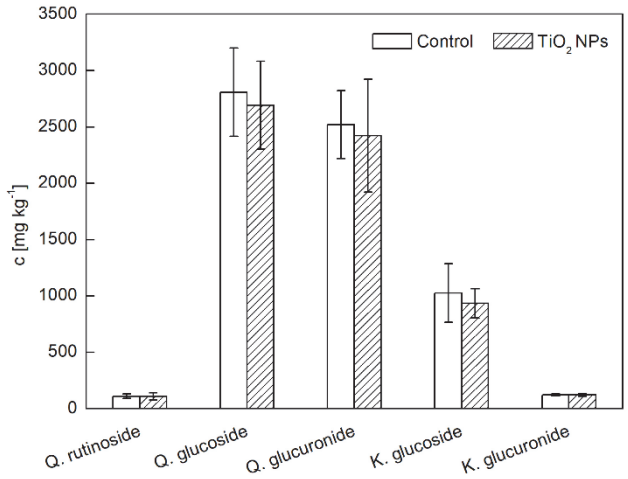


Fig. 6. Comparison of the main flavonol profile of the control and $TiO_2$-treated Cabernet Sauvignon leaves.

translocate from the treated leaves to the untreated ones over a period of three weeks (Table 1). On the other hand, the measured higher concentrations of macronutrients are indicative of the foliar uptake of $TiO_2$. K has a crucial role in many biochemical and physiological processes, such as stomatal movement (Kim *et al.* 2010), water and nutrient transport (Amtmann and Blatt 2009). High K concentrations can be related to the intensive stomatal opening as revealed by our gas-exchange measurements. Treatment-induced stomatal opening is accompanied by elevated water and nutrients uptake which might lead to the selective accumulation of macronutrients in leaves. Indeed, based on the correlation analysis (Table 1), we can conclude that K, P, and Ti correlated significantly with *E*, $g_s$, and $WUE_i$.

**Flavonol profile of leaves**: Flavonols have important role in the defence against ROS and they can protect the photosynthetic apparatus in the leaves (Zhou *et al.* 2016). Therefore, we measured the flavonol content in the leaves of grapevine after treatment with NPs. HPLC-DAD chromatograms of a mixture of various flavonols and an ethanolic extract of control leaves are compared in Fig. 5. Based on their retention time and the recorded spectrum (not shown), the following flavonols were identified and quantified in the leaves: quercetin 3-O-rutinoside, quercetin 3-O-glucoside, quercetin 3-O-glucuronide, kaempferol 3-O-glucoside, and kaempferol 3-O-glucuronide. The predominant component was quercetin 3-O-glucoside (~2,500 mg $kg^{-1}$) while the concentration of quercetin 3-O-rutinoside and kaempferol 3-O-glucuronide was <130 mg $kg^{-1}$. The mean concentration of the main flavonols of the control and treated leaves showed insignificant differences (Fig. 6). However, the comparison of the chromatograms of control and $TiO_2$-treated leaves revealed distinct differences (Fig. 7). It can be clearly seen that the three unknown components with the retention time of 22.8, 26.5, and 31.1 min are significantly reduced or missing from the $TiO_2$-treated leaves, suggesting that these compounds may take part in the defense mechanism against ROS produced photocatalytically.

**Conclusions**: Foliar exposure of *Vitis vinifera* to $TiO_2$ P25 NPs was carried out in field experiments and photosynthetic performance of the leaves was monitored over a period of three weeks. In the presence of ~276 mg($TiO_2$ NPs) $kg^{-1}$(DW), photosynthetic rate decreased while intercellular $CO_2$ concentration and stomatal conductance increased suggesting a nonstomatal limitation of the photosynthesis. $TiO_2$ NPs treatment increased the contents of K, Ca, Mg, P, and B. The elevated K content might

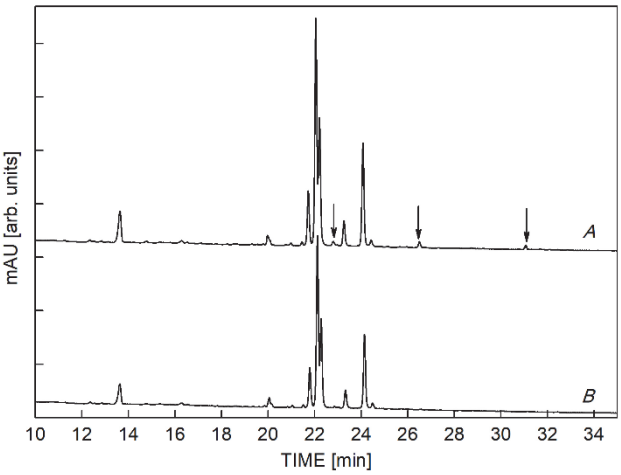


Fig. 7. HPLC-DAD chromatograms of ethanolic extract of (*A*) control and (*B*) $TiO_2$-treated Cabernet Sauvignon leaves. The main differences in the compositions are highlighted with *arrows*.

relate to the observed stomatal opening, and therefore higher transpiration rate of the leaves. After three weeks of NPs exposure, leaf-to-leaf translocation of $TiO_2$ NPs could not be detected but the selective accumulation of macronutrients was indicative for the foliar uptake of NPs. HPLC analysis of flavonoids revealed that some compounds may have active role in the defense mechanism against ROS produced photocatalytically.

## References


Amtmann A., Blatt M.R.: Regulation of macronutrient transport. – New Phytol. **181**: 35-52, 2009.

Anđelković M., Radovanović B., Anđelković A.M. *et al*.: Phenolic compounds and bioactivity of healthy and infected grapevine leaf extracts from red varieties Merlot and Vranac (*V. vinifera* L.). – Plant Food. Hum. Nutr. **70**: 317-323, 2015.

Burke D.J., Zhu S., Pablico-Lansigan M.P., Hewins *et al*.: Titanium oxide nanoparticle effects on composition of soil microbial communities and plant performance. – Biol. Fertil. Soils **50**: 1169-1173, 2014.

Carp O., Huisman C.L., Reller A.: Photoinduced reactivity of titanium dioxide. – Prog. Solid State Ch. **32**: 33-177, 2004.

Castiglione M.R., Giorgetti L., Geri C. *et al*.: The effects of nano-$TiO_2$ on seed germination, development and mitosis of root tip cells of *Vicia narbonensis* L. and *Zea mays* L. – J. Nanopart. Res. **13**: 2443-2449, 2011.

Chacón J.L., García E., Martínez J. *et al*.: Impact of the vine water status on the berry and seed phenolic composition of 'Merlot' (*Vitis vinifera* L.) cultivated in a warm climate: Consequence for the style of wine. – Vitis **48**: 7-9, 2009.

Du W., Sun Y., Ji R. *et al*.: $TiO_2$ and ZnO nanoparticles negatively affect wheat growth and soil enzyme activities in agricultural soil. – J. Environ. Monit. **13**: 822-828, 2011.

Fadeel B., Pietroiusti A., Shvedova A. (ed.): Adverse Effects of Engineered Nanomaterials. Exposure, Toxicology, and Impact on Human Health. Pp. 468. Elsevier Academic Press, New York 2017.

Flamini R., Traldi P.: Grape and wine polyphenols. – In: Desiderio D.M., Nibbering N.M.M. (ed.): Mass Spectrometry in Grape and Wine Chemistry. Pp. 163-214. Wiley & Sons Inc., Hoboken 2010.

Flexas J., Bota J., Escalona J.M. *et al*.: Effects of drought on photosynthesis in grapevines under field conditions: an evaluation of stomatal and mesophyll limitations. – Funct. Plant Biol. **29**: 461-471, 2002.

Flexas J., Scoffoni C., Gago J. *et al*.: Leaf mesophyll conductance and leaf hydraulic conductance: An introduction to their measurement and coordination. – J. Exp. Bot. **64**: 3965-3981, 2013.

Gao J., Xu G., Qian H. *et al*.: Effects of nano-$TiO_2$ on photosynthetic characteristics of *Ulmus elongata* seedlings. – Environ. Pollut. **176**: 63-70, 2013.

Genty B., Briantais J.M., Baker N.R.: The relationship between the quantum yield of photosynthetic electron transport and quenching of chlorophyll fluorescence. – Biochim. Biophys. Acta **990**: 87-92, 1989.

Hashimoto K., Irie H., Fujishima A.: $TiO_2$ photocatalysis: A historical overview and future prospects. – Jpn. J. Appl. Phys. **44**: 8269-8285, 2005.

Hernández I., Alegre L., van Breusegem F. *et al*.: How relevant are flavonoids as antioxidants in plants? – Trends Plant Sci. **14**: 125-132, 2009.

Iacono F., Buccela A., Peterlunger E.: Water stress and rootstock influence on leaf gas exchange of grafted and ungrafted grapevines. – Sci. Hortic.-Amsterdam **75**: 27-39, 1998.

Jacob D.L., Borchardt J.D., Navaratnam L. *et al*.: Uptake and translocation of Ti from nanoparticles in crops and wetland plants. – Int. J. Phytoremediat. **15**: 142-153, 2013.

Keller M.: The Science of Grapevines: Anatomy and Physiology. Pp. 1-377. Academic Press Elsevier, New York 2010.

Kim T.H., Böhmer M., Hu H. *et al*.: Guard cell signal transduction network: advances in understanding abscisic acid, $CO_2$, and $Ca^{2+}$ signaling. – Annu. Rev. Plant Biol. **61**: 561-591, 2010.

Khan M.N., Mobin M., Abbas Z.K. *et al*.: Role of nanomaterials in plants under challenging environments. – Plant Physiol. Bioch. **110**: 194-209, 2017.

Kőrösi L., Dömötör D., Beke S. *et al*.: Antibacterial activity of nanocrystalline $TiO_2$(B) on multiresistant *Klebsiella pneumoniae* strains. – Sci. Adv. Mater. **5**: 1184-1192, 2013.

Kőrösi L., Prato M., Scarpellini A. *et al*.: $H_2O_2$-assisted photocatalysis on flower-like rutile $TiO_2$ nanostructures: Rapid dye degradation and inactivation of bacteria. – Appl. Surf. Sci. **365**: 171-179, 2016.

Larue C., Castillo-Michel H., Sobanska S. *et al*.: Fate of pristine $TiO_2$ nanoparticles and aged paint-containing $TiO_2$ nanoparticles in lettuce crop after foliar exposure. – J. Hazard. Mater. **273**: 17-26, 2014.

Lorenzo M.N., Taboada J.J., Lorenzo J.F., Ramos A.M.: Influence of climate on grape production and wine quality in the Rías Baixas, north-western Spain. – Reg. Environ. Change **13**: 887-896, 2012.

Maxwell K., Johnson G.N.: Chlorophyll fluorescence – a practical guide. – J. Exp. Bot. **51**: 659-668, 2000.

Medrano H., Bota J., Abadía A. *et al*.: Effects of drought on light-energy dissipation mechanisms in high-light-acclimated, field-grown grapevines. – Funct. Plant Biol. **29**: 1197-1207, 2002.

Medrano H., Tomás M., Martorell S. *et al*.: From leaf to whole-plant water use efficiency (WUE) in complex canopies: limitations of leaf WUE as a selection target. – Crop J. **3**: 220-228, 2015.

Ohtani B., Prieto-Mahaney O.O., Li D. *et al*.: What is Degussa (Evonik) P25? Crystalline composition analysis, reconstruction from isolated pure particles and photocatalytic activity test. – J. Photoch. Photobio. A **216**: 179-182, 2010.

Qi M., Liu Y., Li T.: Nano-$TiO_2$ improve the photosynthesis of tomato leaves under mild heat stress. – Biol. Trace Elem. Res. **156**: 323-328, 2013.

Raliya R., Biswas P., Tarafdar J.C.: $TiO_2$ nanoparticle biosynthesis and its physiological effect on mung bean (*Vigna radiata* L.). – Biotechnol. Rep. **5**: 22-26, 2015.

Servin A.D., Morales M.I., Castillo-Michel H. *et al*.: Synchrotron verification of $TiO_2$ accumulation in cucumber fruit: A possible pathway of $TiO_2$ nanoparticle transfer from soil into the food chain. – Environ. Sci. Technol. **47**: 11592-11598, 2013.

Song U., Shin M., Lee G. *et al*.: Functional analysis of $TiO_2$ nanoparticle toxicity in three plant species. – Biol. Trace Elem. Res. **155**: 93-103, 2013.

Taware P.B., Dhumal K.N., Oulkar D.P. *et al*.: Phenolic alterations in grape leaves, berries and wines due to foliar and cluster powdery mildew infections. – Int. J. Pharm. Biol. Sci.

**1**: 1-14, 2010.

Teszlák P., Kocsis M., Gaál K. *et al*.: Regulatory effects of exogenous gibberellic acid ($GA_3$) on water relations and $CO_2$ assimilation among grapevine (*Vitis vinifera* L.) cultivars. – Sci. Hortic.-Amsterdam **159**: 41-51, 2013.

Tomás M., Medrano H., Escalona J.M. *et al*.: Variability of water use efficiency in grapevines. – Environ. Exp. Bot. **103**: 148-157, 2014.

Tortosa I., Escalona J.M., Bota J. *et al*.: Exploring the genetic variability in water use efficiency: Evaluation of inter and intra cultivar genetic diversity in grapevines. – Plant Sci. **251**: 35-43, 2016.

von Caemmerer S., Farquhar G.D.: Some relationships between the biochemistry of photosynthesis and the gas exchange of leaves. – Planta **153**: 376-387, 1981.

Weir A., Westerhoff P., Fabricius L. *et al*.: Titanium dioxide nanoparticles in food and personal care products. – Environ. Sci. Technol. **46**: 2242-2250, 2012.

Yokel R.A. MacPhail R.C.: Engineered nanomaterials: exposures, hazards, and risk prevention. – J. Occup. Med. Toxicol. **6**: 7, 2011.

Yu J., Yu H., Cheng B. *et al*.: Enhanced photocatalytic activity of $TiO_2$ powder (P25) by hydrothermal treatment. – J. Mol. Catal. A-Chem. **253**: 112-118, 2006.

Ze Y., Liu C., Wang L. *et al*.: The regulation of $TiO_2$ nanoparticles on the expression of light-harvesting complex II and photosynthesis of chloroplasts of *Arabidopsis thaliana*. – Biol. Trace Elem. Res. **143**: 1131-1141, 2011.

Zhao Y., Zhang Z., Feng W. (ed.): Toxicology of Nanomaterials. Pp. 407. Wiley-VCH Verlag GmbH & Co. KGaA, Weinheim 2016.

Zhou R., Su W.H., Zhang G.F. *et al*.: Relationship between flavonoids and photoprotection in shade-developed Erigeron breviscapus transferred to sunlight. – Photosynthetica **54**: 201-209, 2016.